THE EFFECT OF RADIATIVE COOLING ON SCALING LAWS OF X-RAY GROUPS AND CLUSTERS

O. MUANWONG,[1] P. A. THOMAS,[1] S. T. KAY,[1] F. R. PEARCE,[2] AND H. M. P. COUCHMAN[3]

ABSTRACT

We have performed cosmological simulations in a ΛCDM cosmology with and without radiative cooling in order to study the effect of cooling on the cluster scaling laws. Our simulations consist of 4.1 million particles each of gas and dark matter within a box size of $100 \, h^{-1}$ Mpc, and the run with cooling is the largest of its kind to have been evolved to $z = 0$. Our cluster catalogs both consist of over 400 objects and are complete in mass down to $\sim 10^{13} \, h^{-1} \, M_\odot$. We contrast the emission-weighted temperature–mass (T_{ew}-M) and bolometric luminosity–temperature (L_{bol}-T_{ew}) relations for the simulations at $z = 0$. We find that radiative cooling increases the temperature of intracluster gas and decreases its total luminosity, in agreement with the results of Pearce et al. Furthermore, the temperature dependence of these effects flattens the slope of the T_{ew}-M relation and steepens the slope of the L_{bol}-T_{ew} relation. Inclusion of radiative cooling in the simulations is sufficient to reproduce the observed X-ray scaling relations without requiring excessive nongravitational energy injection.

Subject headings: cosmology: theory — galaxies: clusters: general

1. INTRODUCTION

The mass of clusters of galaxies[4] is dominated by dark matter. The evolution of the dark matter halo population is now well understood both theoretically (Lacey & Cole 1994) and numerically (Jenkins et al. 2001). The halos themselves are approximately self-similar and may be described in their inner regions by a one-parameter model (Navarro, Frenk, & White 1997) with a concentration parameter that is a slow function of mass. (Note, however, that there are significant deviations from this simple profile in the outer parts of clusters; see Thomas et al. 2001.)

The intracluster medium (ICM) does not share the approximate self-similarity of the dark matter. This is expressed most clearly in the X-ray luminosity–temperature relation. For pure bremsstrahlung emission, the bolometric X-ray luminosity should scale with temperature as $L_X \propto T_X^2$ (the inclusion of line emission flattens this relation), whereas observations indicate a much steeper temperature dependence, especially for low-mass systems (Edge & Stewart 1991; David et al. 1993; Ponman et al. 1996; White, Jones, & Forman 1997; Xue & Wu 2000). At high temperatures, part of this steepening is due to a central cooling flow, but removing the cooling flow component still does not reconcile the observations with the self-similar prediction (Allen & Fabian 1998; Markevitch 1998).

The reason for the departure from self-similarity is that the gas is not as centrally concentrated in clusters as the dark matter, which is best physically expressed as an increase in entropy of the innermost gas (Evrard & Henry 1991; Kaiser 1991; Bower 1997).

The most obvious explanation for this is that there has been some form of energy injection. The amount of energy required depends on the density of the gas at the time when the heating occurred. Lloyd-Davies, Ponman, & Cannon (2000) argue for heating prior to cluster collapse and estimate a value of

0.3 keV per particle. Tozzi & Norman (2001) show that this can be lowered to 0.1 keV per particle by heating at the optimal time (when the gas is at its minimum density), but most other studies that consider heating within collapsed halos require much higher values of 1–3 keV per particle (Wu, Fabian, & Nulsen 2000; Bower et al. 2001; Lowenstein 2000).

There are two likely sources for any excess energy: stellar winds/supernovae and active galactic nuclei (AGNs). It is known for cold dark matter (CDM) models that some feedback of energy into the intergalactic medium must occur in order to prevent the "cooling catastrophe," in which the majority of the baryons in the universe cool and form stars at high redshift (White & Frenk 1991; Cole 1991; Blanchard, Valls-Gabaud, & Mamon 1992). If the heating efficiency is high, supernovae can inject an energy of order 0.3 keV per particle into the intergalactic medium, but they do not do so in an optimal way. Various authors, all of whom consider realistic, but different, models for the buildup of structure, conclude that supernovae are unable to provide the required excess entropy (Valageas & Silk 1999; Wu, Fabian, & Nulsen 2000; Bower et al. 2001). Heating of the intergalactic medium by quasars is also not without its problems, as the heating must occur at just the right time in order not to overly suppress galaxy formation. Alternatively, the heating may arise from AGNs buried within individual galaxies (Bower et al. 2001).

Radiative cooling results in the removal of low-entropy gas in the cluster core and thus leads to an overall increase in temperature of the ICM (Thomas & Couchman 1992). The amount of cooling that takes place in a cooling flow after the final assembly of a cluster is insufficient to explain the observations (Bower et al. 2001), but a more realistic model in which cooling occurs at every stage of the collapse hierarchy can give entropy increases equivalent to an excess energy of 1–2 keV per particle (Wu, Fabian, & Nulsen 2000)—in essence, most of the cooling occurs in galaxy-sized halos before the formation of the cluster. Bryan (2000) has developed a simple model in which low-entropy gas is removed from the cluster core and the surrounding gas is assumed not to have cooled at all. Although this model has obvious deficiencies, it predicts the correct luminosity-temperature relation from 0.5–10 keV.

Simulations of cluster formation including radiative energy loss have been carried out by Pearce et al. (2000). They showed

[1] Astronomy Centre, University of Sussex, Falmer, Brighton, BN1 9QJ, UK; o.muanwong@sussex.ac.uk, p.a.thomas@sussex.ac.uk, s.t.kay@sussex.ac.uk.

[2] Department of Physics, University of Durham, South Road, Durham, DH1 3LE, UK; f.r.pearce@durham.ac.uk.

[3] Department of Physics, McMaster University, Hamilton, Ontario, L8S 4M1, Canada; couchman@physics.mcmaster.ca.

[4] Throughout this Letter we will not distinguish between groups and clusters of galaxies but will use the term clusters to stand for both.

that the gas is slightly heated and that the luminosity is greatly reduced (except in cooling flow clusters), in agreement with expectations. However, the simulations were of limited resolution and covered only a small range in cluster mass. We are now undertaking a program of simulations to extend these results over a wider mass range and to contrast the properties of clusters in different cosmologies. In this Letter, we report results at $z = 0$ from two simulations of a 100 h^{-1} Mpc box in the ΛCDM cosmology, one with and one without radiative cooling.

The simulations and cluster extraction method are described in § 2, and the results are presented in § 3. We summarize our conclusions in § 4.

2. METHOD

2.1. *The Simulations*

We have carried out two simulations with 160^3 particles each of gas and dark matter within cubical volumes of side 100 h^{-1} Mpc. The cosmological parameters were as follows: density parameter, $\Omega_0 = 0.35$; cosmological constant, $\Lambda_0 = \Lambda/3H_0^2 = 0.65$; Hubble parameter, $h = H_0/100$ km s^{-1} Mpc^{-1} = 0.71; baryon density parameter, $\Omega_b h^2 = 0.019$; power spectrum shape parameter, $\Gamma = 0.21$; and a linearly extrapolated rms dispersion of the density fluctuations on a scale 8 h^{-1} Mpc, $\sigma_8 = 0.90$. With these parameters, the gas and dark matter particle masses are approximately 2.6×10^9 and 2.1×10^{10} h^{-1} $M_\odot$, respectively. This mass is below the Steinmetz & White (1997) limit above which numerical heating dominates cooling. The runs were started at redshift $z = 50$ and evolved to the present day, $z = 0$. The gravitational softening was fixed at 50 h^{-1} kpc in comoving coordinates until $z = 1$ and thereafter held constant at 25 h^{-1} kpc in physical coordinates. This softening is sufficient to prevent two-body relaxation (Thomas et al. 2001), and we have checked that the gas and dark matter have similar specific energy profiles in clusters drawn from the nonradiative simulation.

The only difference in the two runs was that one of them included radiative cooling. For this run, we used the cooling tables of Sutherland & Dopita (1993) and assumed a uniform but time-varying metallicity of $Z = 0.3(t/t_0)$ $Z_\odot$, where t/t_0 is the age of the universe in units of the current time. This time-varying metallicity is meant to crudely mimic the gradual enrichment of the ICM by stars, but more importantly it results in a global cooled gas fraction at the end of the simulation of approximately 20%. This is the maximum value inferred from the observations of clusters (Balogh et al. 2001), which means that our simulation will represent the largest effect that cooling alone is likely to have on the ICM.

We use a parallel version of the HYDRA *N*-body/smoothed particle hydrodynamics (SPH) code as described by Couchman, Thomas, & Pearce (1995) and Pearce & Couchman (1997) except that the SPH equations have been modified to use the pairwise artificial viscosity of Monaghan & Gingold (1983); for a test of different SPH formalisms see Thacker et al. (2000). We decouple the hot and cold gas in the manner described by Pearce et al. (1999); see also Ritchie & Thomas 2001 to prevent artificial overcooling of hot gas onto the central cluster galaxies. Groups of 13 or more cold, dense gas particles (with $\delta > 500$ and $T < 12,000$ K) are merged together to form collisionless *galaxy* particles, which can only grow via the accretion of more gas. Not only does this save considerable computational effort, but it also prevents small objects from being artificially disrupted within cluster potentials.

2.2. *The Cluster Catalog*

Initially we identify clusters in our simulation by searching for groups of dark matter particles within an isodensity contour of 200, as described in Thomas et al. (1998). We work with a preliminary catalog of all objects with more than 250 particles, then retain only those that have a total mass within the virial radius exceeding $M_{\rm lim} \approx 1.18 \times 10^{13}$ h^{-1} $M_\odot$, corresponding to 500 particles of each species. The use of a small mass for the preliminary cluster selection ensures that our catalog is complete. We have checked that using a different isodensity threshold, a different selection algorithm, or gas particles instead of dark matter particles to define the cluster, leads to an almost identical cluster catalog—the only difference being the merger or otherwise of a small number of binary clusters.

We define the center of the cluster to be the position of the densest dark matter particle. Because the density parameter of the real universe is not known, we choose to average properties of the clusters within spheres that enclose an overdensity of 200 relative to the critical density (whereas for this cosmology the virial radius corresponds to an overdensity relative to critical of about 110). Our final catalogs consist of 427 and 428 clusters in the radiative and nonradiative simulations, respectively.

2.3. *Cluster X-Ray Properties*

We calculate the bolometric luminosity of each cluster using

$$L_{\rm bol} = \sum_i \frac{m_i \rho_i}{(\mu m_{\rm H})^2} \Lambda(T_i, Z), \qquad (1)$$

where the subscript i denotes the sum over all gas particles within radius r_{200} that have temperatures, $T_i > 10^5$ K, masses m_i, and densities ρ_i; we assume a mean molecular mass $\mu m_{\rm H} = 10^{-24}$ g and an emissivity, $\Lambda[T_i, Z(t)]$, that is the same function used by HYDRA to calculate cooling rates, as discussed in § 2.1. Note that, for temperatures below about 10^7 K, line emission is important and the cooling rates are substantially higher than the contribution from bremsstrahlung alone.

The emission-weighted temperature of each cluster is calculated as

$$T_{\rm ew} = \frac{\sum_i m_i \rho_i \Lambda(T_i, Z) T_i}{\sum_i m_i \rho_i \Lambda(T_i, Z)}. \qquad (2)$$

Many of the smaller clusters in our catalogs have emission-weighted temperatures that are below 0.5 keV, which means that the majority of their emission will emerge at energies that are below the X-ray bands. We do not attempt to calculate the emission in any particular X-ray passband in this Letter but instead quote bolometric luminosities and emission-weighted temperatures.

3. RESULTS

3.1. *Temperature-Mass Relations*

We plot the emission-weighted temperature-mass relation for both cluster samples in Figure 1. Results from the simulations with and without cooling are illustrated using plus signs and filled circles, respectively. The lines are power-law fits to the observational relation as determined by Horner, Mushotzky, & Scharf (1999), using mass estimates from galaxy velocity dis-
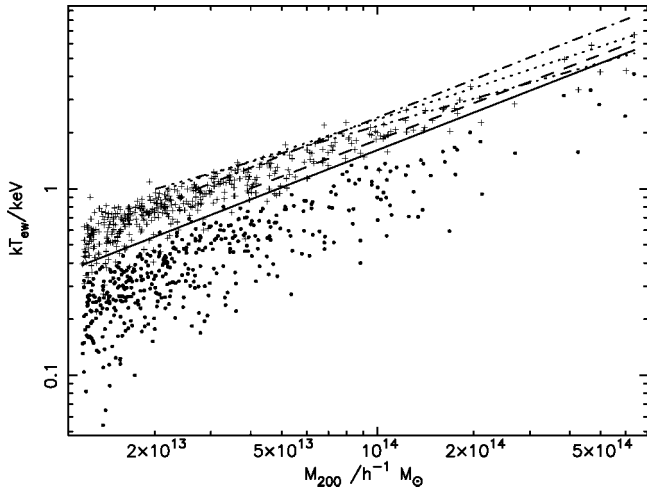
FIG. 1.—Emission-weighted temperature vs. (total) mass within a density contrast of 200. Plus signs and filled circles represent clusters from the simulations with and without radiative cooling, respectively. The various lines are described in the text.
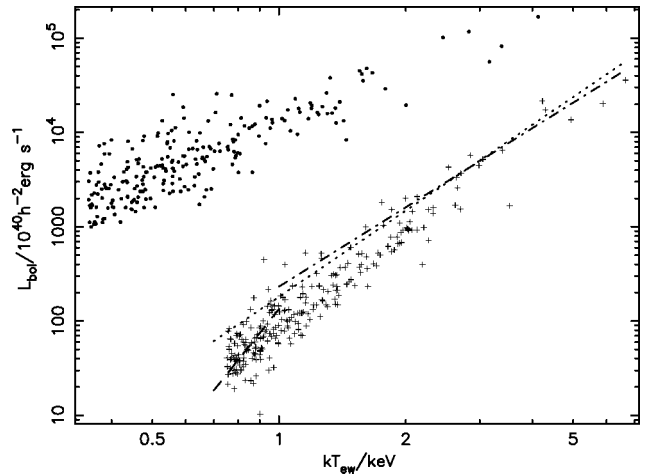

FIG. 2.—Bolometric luminosity–temperature relations for our simulations. Clusters are represented by the same symbols used in Fig. 1, and the lines represent the fits to observational data by Xue & Wu (2000).

persions (*dashed line*), X-ray temperature profiles (*dot-dashed line*), the isothermal β-model (*dotted line*), and the surface brightness deprojection method (*triple-dot–dashed line*).

For the simulation with radiative cooling, the relationship between T_{ew} and M is an approximate power law,

$$kT_{ew} = 1.91 \left(\frac{M_{200}}{10^{14} \ h^{-1} \ M_\odot} \right)^{0.58} \ \text{keV}, \quad (3)$$

and for the simulation without radiative cooling,

$$kT_{ew} = 0.98 \left(\frac{M_{200}}{10^{14} \ h^{-1} \ M_\odot} \right)^{0.67} \ \text{keV}. \quad (4)$$

These should be compared with the virial relation (shown as the solid line in the figure):

$$kT_{vir} = 1.61 \left(\frac{M_{200}}{10^{14} \ h^{-1} \ M_\odot} \right)^{0.67} \ \text{keV}. \quad (5)$$

(Note that no attempt has been made when making these fits to reproduce the observational selection effects. They should therefore be regarded as rough guides rather than precise predictions.) The clusters from the noncooling run mostly have emission-weighted temperatures that are much lower than the virial values. The reason for this is that their emission is dominated by high-density, low-temperature gas in the core of the cluster (this temperature drop in the core is simply due to the fact that the specific energy profile of the gas mimics that of the dynamically dominant dark matter). Small fluctuations in the core properties of the clusters (which are not well resolved by our simulations) lead to a large scatter in predicted temperatures. It is important to note that these nonradiative simulations do not provide sensible predictions for the observed properties of real clusters—the core gas has a short cooling time and would not in reality persist in the ICM for the lifetime of the cluster.

We note that our nonradiative T_{ew}-M relation has a lower normalization than found by Thomas et al. (2001) for simulations in the τCDM cosmology because there it was assumed

that the emission is purely bremsstrahlung, which underestimates cooling rates below 10^7 K and places less weight on the innermost region of clusters.

In contrast to the nonradiative run, the clusters from the radiative simulation have emission-weighted temperatures that show less scatter and that exceed the virial values. The reason for this is that the core gas has cooled to low temperatures and has been removed from the ICM, leaving behind higher entropy, higher temperature gas—an effect that is more pronounced in lower mass clusters. The emission is no longer dominated by the core and is well resolved by our simulations. The clusters provide an adequate fit to the observational data given the large uncertainty in the latter, as evidenced by the various lines in Figure 1.

3.2. *Luminosity-Temperature Relations*

Figure 2 illustrates X-ray luminosity–temperature relations for both simulations, again using plus signs and filled circles for radiative and nonradiative clusters, respectively. We have trimmed the original catalogs by selecting clusters only with temperatures above 0.35 and 0.75 keV for the nonradiative and radiative cooling catalogs, respectively, to assure completeness in temperature. The lines illustrate best-fit power-law relations as determined by Xue & Wu (2000) for their collected group sample (*dashed line*), cluster sample (*dot-dashed line*), and combined sample (*dotted line*). (Note that the units for the normalization of the relations in Table 2 of Xue & Wu 2000 are misquoted and should be a factor of 10 larger, in agreement with their Table 1 and Fig. 1.)

A power-law fit to results from the radiative simulation gives

$$L_{bol} = 9.0 \times 10^{41} \left(\frac{T_{ew}}{1 \ \text{keV}} \right)^{3.3} \ h^{-2} \ \text{ergs s}^{-1}, \quad (6)$$

and for the nonradiative simulation

$$L_{bol} = 1.2 \times 10^{44} \left(\frac{T_X}{1 \ \text{keV}} \right)^{1.9} \ h^{-2} \ \text{ergs s}^{-1}. \quad (7)$$

(As stated in § 3.1, these fits should not be taken as precise

calibrations.) Again, both the slope and normalization differ between the two simulations. The nonradiative simulation gives a slope close to 2, as predicted by self-similar scaling relations (the relation is slightly flatter because of the inclusion of line emission). However, the radiative simulation gives a significantly steeper slope of 3.3. The normalization of the relation is around a factor of 10–100 lower in the radiative simulation than in the nonradiative simulation. Qualitatively, these differences are the same as were found by Pearce et al. (2000) for a smaller cluster sample. The high-entropy gas that replaces cooled material in the radiative simulation is hotter and less dense than the gas in the nonradiative simulation. The change in density has the greater effect, since the X-ray emissivity is a slow function of temperature but is proportional to the square of the gas density. The combination of the increase in temperature and the decrease in luminosity of the clusters causes the substantial shift in the L_{bol}-T_{ew} relation.

The results from the radiative simulation are in good agreement with the best-fit relations of Xue & Wu (2000). If anything, we predict luminosities that are a factor of 2–3 too low, although there is still significant uncertainty in the observational determinations.

4. CONCLUSIONS

In this Letter, we have presented results from an ongoing program to measure the evolution of X-ray cluster properties for a range of physical and cosmological models. Specifically, we have presented the current-day ($z = 0$) emission-weighted temperature–mass (T_{ew}-M) and bolometric luminosity–temperature (L_{bol}-T_{ew}) relations from two simulations of a ΛCDM cosmology, one with and one without radiative cooling.

The T_{ew}-M relation is significantly different in nonradiative and radiative simulations, with the latter in reasonable agreement with observational determinations. In the noncooling simulation, the emission is dominated by cold, dense gas in the cores of the clusters; radiative cooling removes this gas from the ICM (converting it into stars) and replaces it with higher entropy, hotter material. This effect is more prevalent in lower mass systems and so flattens the temperature-mass relation.

The L_{bol}-T_{ew} relation is also significantly different between the two simulations. The high-entropy material in the radiative simulation is less dense than the material it replaces and causes the X-ray luminosity of clusters to decrease by around a factor of 100 at $T_{ew} = 1$ keV. The slope of the relation in the nonradiative simulation is 1.9, similar to self-similar predictions. However, the slope of the radiative relation is significantly steeper, 3.3, again due to the differential effect of cooling with halo temperature. The radiative simulation is in much closer agreement with the observations, both in the slope and normalization of the relation.

In this Letter, we have used bolometric luminosities and emission-weighted temperatures. For the low-temperature clusters found in the nonradiative simulations, these will differ significantly from properties measured in any particular X-ray band. However, we wish to emphasize that to attempt to correct for this is misleading, as the use of such simulations is wrong in principle—the low-entropy gas in the cores of these clusters has a short cooling time and will not be present in real systems.

The global fraction of cooled gas (and stars) in the radiative simulation, 20%, is higher than suggested by observations of the K-band galaxy luminosity function (Balogh et al. 2001). More importantly, the fraction of cooled gas within the clusters varies between about one-third and two-thirds with decreasing mass. While these values are not convincingly ruled out by observations, most people would also regard these as high values—in which case our simulation can be treated as an upper bound on the effect of radiative cooling.

In this Letter, we have deliberately ignored the effect of nongravitational heating on the gas. In reality, we know that there must be heating associated with star formation and metal enrichment of the ICM. This will raise the entropy of the gas and reduce the amount of cooling that is required to match the observations. However, we do not regard the case for significant heating by AGNs or very efficient supernovae feedback as proven.

REFERENCES

Allen, S. W., & Fabian, A. C. 1998, MNRAS, 297, L57
Balogh, M. L., Pearce, F. R., Bower, R. G., & Kay, S. T. 2001, MNRAS, submitted (astro-ph/0104041)
Blanchard, A., Valls-Gabaud, D., & Mamon, G. A. 1992, A&A, 264, 365
Bower, R. G. 1997, MNRAS, 288, 355
Bower, R. G., Benson, A. J., Lacey, C. G., Baugh, C. M., Cole, S., & Frenk, C. S. 2001, MNRAS, in press (astro-ph/0006109)
Bryan, G. L. 2000, ApJ, 544, L1
Cole, S. 1991, ApJ, 367, 45
Couchman, H. M. P., Thomas, P. A., & Pearce, F. R. 1995, ApJ, 452, 797
David, L. P., Slyz, A., Jones, C., Forman, W., & Vrtilek, S. D. 1993, ApJ, 412, 479
Edge, A. C., & Stewart, G. C. 1991, MNRAS, 252, 414
Evrard, A. E., & Henry, J. P. 1991, ApJ, 383, 95
Horner, D. J., Mushotzky, R. F., & Scharf, C. A. 1999, ApJ, 520, 78
Jenkins, A., Frenk, C. S., White, S. D. M., Colberg, J. M., Cole, S., Evrard, A. E., Couchman, H. M. P., & Yoshida, N. 2001, MNRAS, 321, 372
Kaiser, N. 1991, ApJ, 383, 104
Lacey, C., & Cole, S. 1994, MNRAS, 271, 676
Lloyd-Davies, E. J., Ponman, T. J., & Cannon, D. B. 2000, MNRAS, 315, 689
Lowenstein, M. 2000, ApJ, 532, 17
Markevitch, M. 1998, ApJ, 504, 27
Monaghan, J. J., & Gingold, R. A. 1983, J. Comput. Phys., 52, 375

Navarro, J. F., Frenk, C. S., & White, S. D. M. 1997, ApJ, 490, 493
Pearce, F. R., & Couchman, H. M. P. 1997, NewA, 2, 411
Pearce, F. R., et al. 1999, ApJ, 521, L99
Pearce, F. R., Thomas, P. A., Couchman, H. M. P., & Edge, A. C. 2000, MNRAS, 317, 1029
Ponman, T. L., Bourner, P. D. J., Ebeling, H., & Böhringer, H. 1996, MNRAS, 283, 690
Ritchie, B. W., & Thomas, P. A. 2001, MNRAS, 323, 743
Steinmetz, M., & White, S. D. M. 1997, MNRAS, 288, 545
Sutherland, R. S., & Dopita, M. A. 1993, ApJS, 88, 253
Thacker, R. J., Tittley, E. R., Pearce, F. R., Couchman, H. M. P., & Thomas, P. A. 2000, MNRAS, 319, 619
Thomas, P. A., et al. 1998, MNRAS, 296, 1061
Thomas, P. A., & Couchman, H. M. P. 1992, MNRAS, 257, 11
Thomas, P. A., Muanwong, O., Pearce, F. R., Couchman, H. M. P., Edge, A. C., Jenkins, A., & Onuora, L. 2001, MNRAS, in press (astro-ph/0007348)
Tozzi, P., & Norman, C. 2001, ApJ, 546, 63
Valageas, P., & Silk, J. 1999, A&A, 350, 725
White, D. A., Jones, C., & Forman, W. 1997, MNRAS, 292, 419
White, S. D. M., & Frenk, C. S. 1991, ApJ, 379, 52
Wu, K. K. S., Fabian, A. C., & Nulsen, P. E. J. 2000, MNRAS, 318, 889
Xue, Y.-J., & Wu, X.-P. 2000, ApJ, 538, 65